Rapid Communications

Nonlocal thermoelectricity in a topological Andreev interferometer

Gianmichele Blasi,[1,*] Fabio Taddei,[1] Liliana Arrachea,[2] Matteo Carrega,[1,3] and Alessandro Braggio[1,†]

[1]*NEST, Scuola Normale Superiore and Instituto Nanoscienze-CNR, I-56126 Pisa, Italy*

[2]*International Center for Advanced Studies, ECyT-UNSAM and ICIFI, Campus Miguelete, 25 de Mayo y Francia, 1650 Buenos Aires, Argentina*

[3]*SPIN-CNR, Via Dodecaneso 33, 16146 Genova, Italy*

(Received 20 August 2020; accepted 4 December 2020; published 18 December 2020)

We discuss the phase-dependent nonlocal thermoelectric effect in a topological Josephson junction in contact with a normal-metal probe. We show that, due to the helical nature of topological edge states, nonlocal thermoelectricity is generated by a purely Andreev interferometric mechanism. This response can be tuned by imposing a Josephson phase difference, through the application of a dissipationless current between the two superconductors, even without the need of applying an external magnetic field. We discuss in detail the origin of this effect and we also provide a realistic estimation of the nonlocal Seebeck coefficient which turns out to be of the order of a few μV/K at temperatures of a few kelvin.

DOI: 10.1103/PhysRevB.102.241302

Introduction. Prominent topics in hybrid superconducting quantum technologies concern thermal management [1–3] and thermoelectricity [4–11]. These represent novel functionalities for quantum sensing [12–14], entanglement manipulation [15], and thermal engines [16–20].

Usually, finite thermoelectric response appears in hybrid superconducting systems only when the particle-hole symmetry, encoded in the Bogoliubov–de Gennes (BdG) Hamiltonian, is broken, e.g., by means of ferromagnetic correlations [21–25] or by exploiting nonlinearities [10,11,26]. Recently, mechanisms able to generate *nonlocal* thermoelectricity have been predicted in Cooper pair splitters [8,9] and Andreev interferometers [27–30], and experimentally investigated [31–34]. We have demonstrated [35] that a Josephson junction based on a two-dimensional (2D) topological insulator (TI) [36–40] threaded by a magnetic flux with one edge attached to a normal metallic probe [41] presents nonlocal thermoelectricity when a temperature difference is applied between the two superconducting leads. The responsible mechanism is the so-called Doppler shift induced by the magnetic flux in the junction, which has an effect akin to a Zeeman splitting in the two spin-polarized members of the Kramer pair of the 2D TI [42].

In this work, we show that a phase bias *alone* in a topological Josephson junction is sufficient to establish finite nonlocal thermoelectricity. This is very appealing since, differently from the mechanism of Ref. [35], the present one takes place without the necessity of a magnetic field. Its origin is the helical property of edge states and solely relies on the superconducting Andreev interferometric effect. Importantly, such thermoelectric response disappears when both edges are connected to the probe or when the TI is replaced by normal channels. Hence, it constitutes a peculiar feature of the helical nature of the 2D TI. We argue that, with state-of-the-art technologies, the corresponding nonlocal Seebeck coefficient turns out to be of the order of a few μV/K at temperatures of a few kelvin.

Model. We consider the topological Josephson junction depicted in Fig. 1, which consists of two superconducting electrodes placed on top of a 2D TI at a distance L. The two electrodes induce superconducting correlations on the edge states via proximity effect [42,43]. The width of the TI strip is assumed to be large enough such that upper and lower edges are decoupled, and we focus only on the upper edge. The system is described by the following BdG Hamiltonian:

$$\mathcal{H} = \begin{pmatrix} H(x) & i\sigma_y\Delta(x) \\ -i\sigma_y\Delta(x)^* & -H(x)^* \end{pmatrix}, \tag{1}$$

expressed in the Nambu basis $(\psi_\uparrow, \psi_\downarrow, \psi_\uparrow^*, \psi_\downarrow^*)^T$ with spin $\uparrow$ and $\downarrow$ collinear with the natural spin-quantization axis of the TI edge along the z direction, where $H(x) = v_F(-i\hbar\partial_x)\sigma_z - \mu\sigma_0$ with $-H(x)^*$ being its time-reversal partner. The Fermi velocity is v_F, μ is the chemical potential, and σ_i are the Pauli matrices. We consider rigid boundary conditions with order parameter $\Delta(x) = \Delta_0[\Theta(-x)e^{i\phi_{S_L}} + \Theta(x-L)e^{i\phi_{S_R}}]$, where $\Theta(x)$ is the step function, Δ_0 is the proximity induced gap, and $\phi \equiv \phi_{S_R} - \phi_{S_L}$ is the gauge invariant Josephson phase difference between the two superconductors. A normal-metal probe N, such as a scanning tunneling microscopy (STM) tip [44–47], is directly contacted to the upper edge on the point x_0 (see Fig. 1) and modeled by an energy- and spin-independent transmission amplitude t.

Charge current at the probe. In the setup depicted in Fig. 1, a voltage bias V_N is applied between the probe N at the temperature T_N and the superconducting electrodes (grounded) [48]. In this configuration the only thermal bias that gives rise to a nonlocal electric response in the probe is $\delta T = T_{S_L} - T_{S_R}$ imposed between the superconductors. By using the scattering approach [49–51] one can write the charge current J_N^c flowing

*gianmichele.blasi@sns.it
†alessandro.braggio@nano.cnr.it

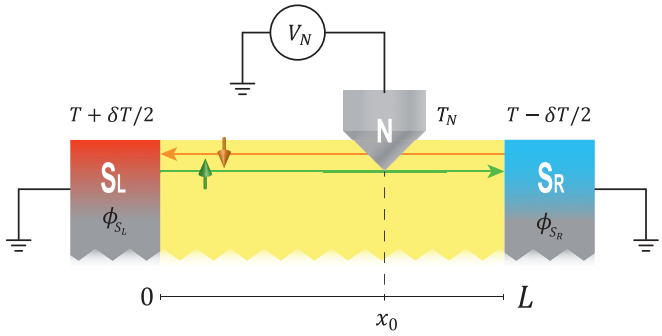

FIG. 1. A helical Kramers pair of edge states of the quantum spin Hall effect is contacted by two superconductors at different temperatures $T_{S_L} = T + \delta T/2$ and $T_{S_R} = T - \delta T/2$, and a phase difference $\phi \equiv \phi_{S_R} - \phi_{S_L}$. A bias voltage V_N is applied to the normal-metal probe at temperature T_N and coupled to the edge at the point $0 \leqslant x_0 \leqslant L$, with L the length of the junction.

in the probe as follows:

$$J_N^c = \frac{2}{h} \sum_{j,\alpha,\beta} \int_0^\infty d\epsilon\, \alpha e \big[f_N^\alpha(\epsilon) - f_j^\beta(\epsilon) \big] P_{N,j}^{\alpha,\beta}(\epsilon, \phi), \qquad (2)$$

where $\alpha, \beta = +$ stand for quasiparticle (QP), $\alpha, \beta = -$ for quasihole (QH), and with j running over leads indices (S_L, S_R, and N). In Eq. (2) we consider the chemical potentials of the grounded superconductors as reference for the energies. The current depends on the generalized Fermi distributions $f_j^\alpha(\epsilon) = \{e^{(\epsilon - \alpha e V_j)/k_B T_j} + 1\}^{-1}$, where T_j and V_j are, respectively, the temperature and the voltage at the lead j. Notice that when $V_j = 0$ (for the grounded superconductors $V_{S_L} = V_{S_R} = 0$), $f_j^-(\epsilon) = f_j^+(\epsilon)$. The scattering coefficients $P_{i,j}^{\alpha,\beta}(\epsilon, \phi)$, with $i, j = N, S_L, S_R$, represent the reflection ($i = j$) or transmission ($i \neq j$) probabilities of a quasiparticle of type β in lead j to a quasiparticle of type α in lead i [51].

Symmetries. As a consequence of the helical nature of the edge states, the fact that the probe is not spin polarized and for superconductors with equal gap, it is found that the scattering coefficients $P_{i,j}^{\alpha,\beta}(\epsilon, \phi)$ do not depend on the probe position. This is because each path taken by particles comes in pairs with its symmetric one (obtained by exchanging left and right). Hence, all the results discussed hereafter do not depend on x_0. Furthermore, it can be shown that peculiar *nonlocal* symmetries hold for the scattering coefficients of Eq. (2) between the probe and the left/right superconductors, namely, $P_{NS_{L/R}}^{\alpha\beta}(\epsilon, \phi) = P_{NS_{R/L}}^{-\alpha-\beta}(\epsilon, \phi)$ and $P_{NS_{L/R}}^{\alpha\beta}(\epsilon, \phi) = P_{NS_{L/R}}^{-\alpha-\beta}(\epsilon, -\phi)$, while the reflection coefficients at the probe N satisfy the relation $P_{NN}^{\alpha\beta}(\epsilon, \phi) = P_{NN}^{-\alpha-\beta}(\epsilon, \phi)$ between QP and QH states.

Nonlocal thermoelectric response. By exploiting the aforementioned symmetry relations, one can write the charge current at the probe J_N^c in the following form:

$$J_N^c = \frac{2}{h} \int_0^\infty d\epsilon \, \{ F_N^-(\epsilon) A(\epsilon, \phi) - F_S^-(\epsilon) [Q(\epsilon, \phi) - Q(\epsilon, -\phi)] \}, \qquad (3)$$

where in the first term we recognize the Fermi function differences for normal probe $F_N^- \equiv f_N^+ - f_N^-$ weighted with a

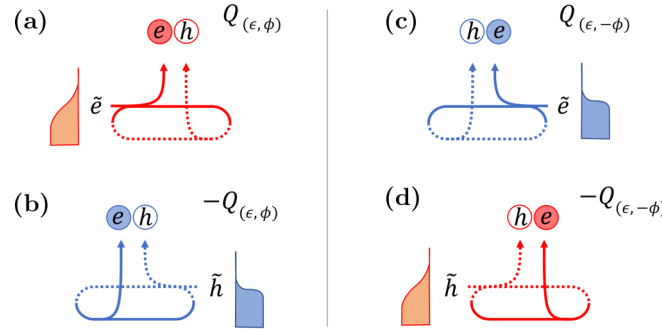

FIG. 2. Resonant processes describing the transfer of the charge Q from the superconducting leads S_L, S_R into the probe N. $\tilde{e}$, $\tilde{h}$ label, respectively, QP and QH at the superconducting leads. Solid and dashed lines correspond to the trajectories traveled by electrons and holes, respectively. Red (blue) corresponds to processes originated at the hot (cold) lead S_L (S_R) whose Fermi distribution $f_{S_L} = f_{S_L}^\pm$ ($f_{S_R} = f_{S_R}^\pm$) is sketched on the side. In (a) and (b) are depicted the processes of QP and QH injected from S_L and S_R, respectively, and corresponding to a transfer of the opposite amount of charge $Q(\epsilon, \phi)$ (a) and $-Q(\epsilon, \phi)$ (b). In (c) and (d) are depicted the dual processes obtained by inverting the lead of injection ($S_L \rightleftarrows S_R$) and the sign of $\phi \to -\phi$.

scattering coefficient

$$A(\epsilon, \phi) = e(N_N^+ - P_{NN}^{++} + P_{NN}^{+-}) = e(N_N^- - P_{NN}^{--} + P_{NN}^{-+}) \qquad (4)$$

that represents the electronic charge transferred from the probe N into the edge, being $P_{NN}^{\pm\pm}$ normal reflections, $P_{NN}^{\pm\mp}$ the Andreev ones, and $N_N^{+(-)}$ the number of open channels for electrons (holes) at the probe. The second term instead contains the Fermi function differences between the two superconductors $F_S^- \equiv f_{S_L}^\pm - f_{S_R}^\mp$ which are nonzero when a thermal bias $\delta T \neq 0$ is applied between the superconductors. The function F_S^- is weighted with the odd parity component, with respect to ϕ, of the function

$$Q(\epsilon, \phi) = e\big(P_{NS_L}^{++} - P_{NS_L}^{-+}\big) = -e\big(P_{NS_R}^{+-} - P_{NS_R}^{--}\big). \qquad (5)$$

A visualization of the meaning of the quantity Q is given in Fig. 2 where we sketch the resonant processes where a QP or QH is injected from right or left superconductors and is transferred after multiple resonant Andreev processes to the probe as an electron (solid) or a hole (dashed). In particular, Q represents the net electronic charge transferred into the probe N when a QP is injected from S_L [see Fig. 2(a)]. The symmetries show that a QH injected from the right superconductor S_R brings exactly the same amount of charge, with opposite sign [second identity of Eq. (5)] as represented in Fig. 2(b). Alongside these processes [represented in Figs. 2(a) and 2(b)], there are also dual processes, depicted in Figs. 2(c) and 2(d), which correspond to the same amount of transferred charge given in Eq. (5) obtained by exchanging the side of injection (i.e., $S_L \rightleftarrows S_R$) and inverting the sign of $\phi \to -\phi$.

We now discuss the physical consequence of the result reported in Eq. (3). When $V_N = 0$ there is no contribution from the Fermi functions of the normal probe (i.e., $F_N^- = 0$) because $f_N^+(\epsilon) = f_N^-(\epsilon)$. Since T_N does not enter these expressions, the possibility of inducing *local* thermoelectricity

by means of a thermal bias between the TI and the probe is ruled out. This is particularly important at the experimental level since the temperature of the probe does not need to be controlled during the measurement of nonlocal thermoelectricity. The only thermoelectric response in the probe is the *nonlocal* one when a thermal bias between the two superconductors δT is applied, i.e., $F_S^- = f_{S_L}^{\pm}(\epsilon) - f_{S_R}^{\mp}(\epsilon) \neq 0$. This nonlocal thermoelectric response [see Eq. (3)] is determined by the integral over the energies of the odd parity component in ϕ of the function $Q(\epsilon,\phi)$, i.e., $Q(\epsilon,\phi) - Q(\epsilon,-\phi)$. If $\phi = 0$, one cannot have nonlocal thermoelectricity. The physical reason for this result comes from the exact cancellation of the contributions of the processes represented in Fig. 2: in particular, (a) cancels with (d) and (b) with (c).

Phase-dependent thermoelectricity. Here we concentrate on the action of the Josephson phase bias ϕ showing that it is responsible for the generation of nonlocal thermoelectricity in the probe due to a peculiar Andreev interferometric effect associated to the helical nature of the edge, as pictorially sketched in Fig. 2. This can be rationalized looking at the analytical expressions of the quantities A and Q of Eqs. (4) and (5) [51]:

$$A(\epsilon,\phi) = \sum_{\sigma=\pm} \frac{2e|t|^4\Theta(\Delta-\epsilon)}{1+|r|^4+2|r|^2\cos\left[2\pi\frac{L\epsilon}{\xi\Delta}+\sigma\phi+2\arcsin\left(\frac{\epsilon}{\Delta}\right)\right]} + \sum_{\sigma=\pm} \frac{e[g(\epsilon)+1][g(\epsilon)-|r|^2]|t|^2\Theta(\epsilon-\Delta)}{g(\epsilon)^2+|r|^4-2g(\epsilon)|r|^2\cos\left(2\pi\frac{L\epsilon}{\xi\Delta}+\sigma\phi\right)}, \tag{6}$$

$$Q(\epsilon,\phi) = \frac{e[g(\epsilon)-1][g(\epsilon)-|r|^2]|t|^2\Theta(\epsilon-\Delta)}{g(\epsilon)^2+|r|^4-2g(\epsilon)|r|^2\cos\left(2\pi\frac{L\epsilon}{\xi\Delta}-\phi\right)}, \tag{7}$$

where $g(\epsilon) = (\epsilon/\Delta + \sqrt{\epsilon^2/\Delta^2-1})^2$, $|r|^2 = 1-|t|^2$, and $\xi = \hbar v_F/\pi\Delta$ is the superconducting coherence length. Notice that Eq. (6) consists of two parts, each related to the subgap (first term) and supragap (second term) processes, while Eq. (7) contains only the supragap contribution. In particular, from Eq. (7), it emerges that $Q(\epsilon,\phi)$ has no definite symmetry in ϕ for $L \neq 0$ so that one would expect a finite nonlocal thermoelectric response. The interferential nature of the phenomena can be better enlightened by investigating the behavior of the Onsager coefficients in the linear response regime as we discuss next.

Linear response regime. In the linear response regime, for $\delta T, V_N \to 0$, the temperature of the probe can be chosen as the average temperature of the superconducting leads, i.e., $T_N = (T_{S_L} + T_{S_R})/2 = T$. With this choice the heat current in the probe is zero while it flows only between the two superconductors. So the relevant responses are the charge current flowing in the probe J_N^c and the heat current flowing in one (say the left) superconductor [49–51]

$$J_{S_L}^h = \frac{2}{h}\sum_{j,\alpha,\beta}\int_0^\infty d\epsilon\,\epsilon\left[f_{S_L}^\alpha(\epsilon) - f_j^\beta(\epsilon)\right]P_{S_L,j}^{\alpha,\beta}(\epsilon,\phi). \tag{8}$$

The electric current flowing between the superconducting leads is mainly dominated by the Josephson (equilibrium) current determined by the superconducting phase difference, unless it overcomes the value of the critical current of the junction. Hence, no linear thermovoltage response can take place between the two superconductors. Quantitatively, the linear response regime is thus characterized by the following relations [6,8,9,16,52,53]:

$$\begin{aligned} J_N^c &= L_{11}(V_N/T) + L_{12}(\delta T/T^2), \\ J_{S_L}^h &= L_{21}(V_N/T) + L_{22}(\delta T/T^2). \end{aligned} \tag{9}$$

Interestingly, although the configuration contains three terminals, the relevant driving affinities for nonlocal thermoelectric response of this setup are only two, namely, V_N/T and $\delta T/T^2$. Hence, the Onsager matrix, with entries L_{ij}, is effectively 2×2 [16,52–55]. In this effective formulation one should be reminded that L_{12} and L_{21} are *nonlocal* thermoelectrical coefficients. In Fig. 3 the Onsager coefficients are plotted as functions of ϕ/π and the length measured as L/ξ. In Figs. 3(a), 3(b), and 3(c) we plot, respectively, the local

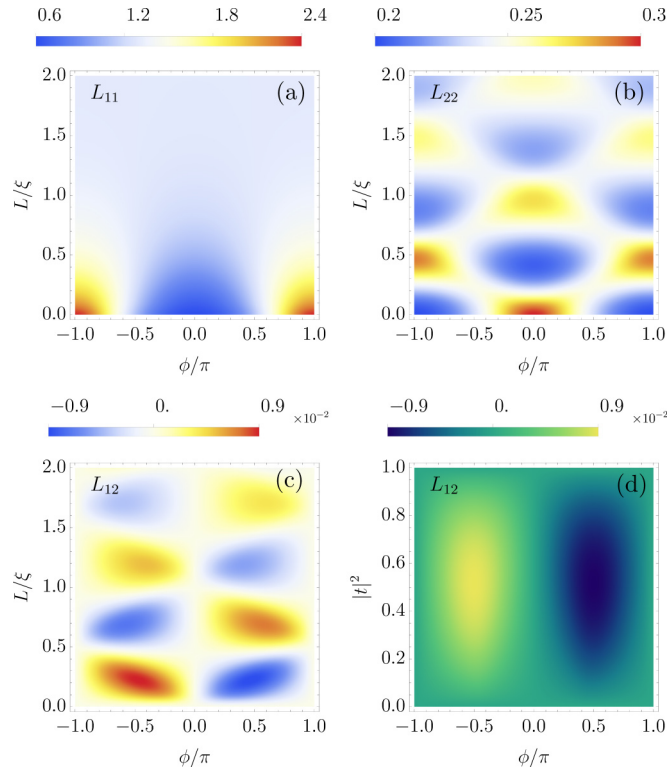

FIG. 3. Phase dependence of the Onsager coefficients. L_{11} (a), L_{22} (b), and $L_{12} = -L_{21}$ (c) as functions of ϕ/π and the junction length L/ξ for $|t|^2 = 0.5$. (d) L_{12} as a function of ϕ/π and coupling parameter $|t|^2$ with the junction length $L/\xi = 0.25$ (for which it is maximal). Such quantities are taken at $T/T_C = 0.4$ and normalized as follows: $L_{11}/(G_0T)$, $L_{22}/(G_TT^2)$, and $L_{12}/(\sqrt{G_0G_TT^3})$, with $G_0 = 2e^2/h$ and $G_T = (\pi^2/3h)k_B^2T$ being, respectively, the electrical conductance quantum and the thermal conductance quantum.

Onsager coefficients L_{11}, L_{22}, and the nonlocal thermoelectrical coefficient L_{12} setting the strength of the coupling with the probe at an intermediate value [56] $|t|^2 = 0.5$ and the temperature fixed at $T/T_C = 0.4$ (the highest temperature at which the induced gap of the right and left superconductors remain constant and equal to Δ_0), where T_C is the critical temperature. Notice that, by exploiting the aforementioned symmetries of the scattering coefficients, it can be shown that the off-diagonal nonlocal coefficients satisfy a generalized nonlocal Onsager symmetry relation $L_{12}(\phi) = L_{21}(-\phi) = -L_{21}(\phi)$, similarly to the case discussed in Ref. [35].

We observe that L_{11} (which is proportional to the conductance at the probe), is an even function [57] of ϕ and, for small length $L \ll \xi$, presents a minimum for $\phi \approx 0$ and a maximum at $\phi \approx \pm\pi$. Increasing the length L, the conductance becomes featureless and flat due to an effective averaging between the (increasing) number of available states involved in the transport. More interesting, instead, is the behavior of L_{22} and L_{12} which present a periodicity of one coherence length ξ as functions of the length of the junction [43]. This periodicity is determined by the oscillatory change of available states at energies $\epsilon \gtrsim \Delta$, which dominate the spectral contribution to the transport window, oscillating between a maximum to a minimum when the junction length changes by one ξ length. This effect is not present in L_{11} since it is mostly determined by subgap states given by the Andreev contributions. Remarkably, this oscillatory behavior affects also the thermal conductance ($\propto L_{22}$) which crucially differs from the nonlocal thermoelectric coefficient ($\propto L_{12}$) since the first is even with the phase bias ϕ while the latter is odd [57,58] [see Eq. (3)]. The different symmetry in ϕ is due to the fact that QPs and QHs contribute with the same sign to the heat transport but with opposite sign to the thermoelectric current.

In Fig. 3(d) we show how L_{12} changes with the coupling parameter $|t|^2$, keeping the length of the junction fixed to $L/\xi = 0.25$ [for which it is maximal; see Fig. 3(c)]. It emerges that the absolute value of the nonlocal Onsager coefficient L_{12} reaches its maximum for an intermediate value of the coupling parameter (i.e., $|t|^2 \approx 0.5$), while it is either zero when $|t|^2 \to 0$ (when the probe is decoupled) or $|t|^2 \to 1$ (when the two superconductors are mutually decoupled).

We stress that the appearance of this nonlocal linear thermoelectric effect is a unique feature of our hybrid topological Josephson junction when the probe is contacted with just one helical edge of the TI. Such thermoelectric response, instead, disappears when both edges are connected to the probe or when the TI is replaced by normal spinful channels. More precisely, we verified that in the case of a standard S-N-S junction in contact with a normal-metal probe, $L_{12} = L_{21} = 0$.

As a final remark, it is important to give a realistic estimation of the strength of the thermoelectrical effect we are discussing. In this regard, we compute the nonlocal Seebeck coefficient $S = (1/T)L_{12}/L_{11}$ [52] as a function of ϕ (see Fig. 4). As a consequence of the latter relation, we notice that S, being proportional to L_{12}, stems from Andreev interference effetcs. In order to make realistic predictions in a wide temperature range, here we also include the temperature dependence of the gap order parameter [59,60]. Figure 4(a)

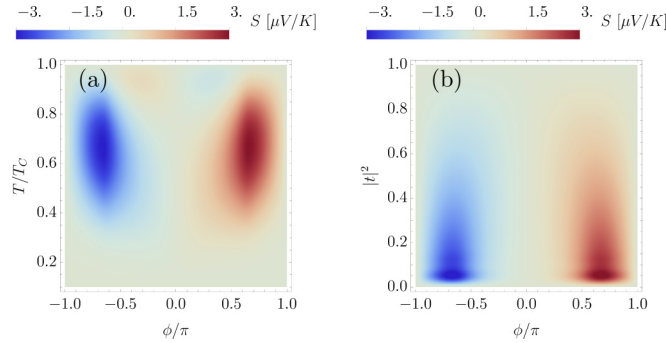

FIG. 4. (a) Nonlocal Seebeck coefficient as a function of ϕ/π versus T/T_C for $|t|^2 = 10^{-2}$. (b) Nonlocal Seebeck coefficient as a function of ϕ/π versus the probe coupling $|t|^2$ for $T/T_C = 0.7$. Both (a) and (b) have been obtained for the same length $L/\xi = 0.25$.

shows that the nonlocal Seebeck coefficient grows with the operating temperature and reaches a maximum of 3 μV/K roughly at $T/T_C \approx 0.7$ for $\phi/\pi \approx \pm 0.6$. At higher temperatures the gap closes reducing the nonlocal thermoelectricity, hence confirming the fundamental role of the superconducting state. Figure 4(b) (obtained for $T/T_C = 0.7$) shows how the nonlocal Seebeck effect scales with the probe coupling $|t|^2$ as a result of the scaling of the ratio L_{12}/L_{11}. At small coupling $|t|^2 \approx 10^{-2}$ it returns highest values. Notably these values of the phase-dependent nonlocal Seebeck coefficient are roughly 6% of the values determined by the Doppler shift mechanism proposed in Ref. [35]. The advantage in the present case, is that there is no need of any magnetic field since it is enough to impose a dissipationless current between the two superconductors to induce the phase bias ϕ. This experimental protocol seems quite attractive due to its simplicity and the absence of any spurious Nernst effect [61–64].

In Fig. 4 we considered the length of the junction $L/\xi = 0.25$. This situation is reasonable assuming a STM tip with state-of-the-art size of 100 nm and a coherence length ξ in the proximized TI of the order of 600 nm [65,66]. Further, this choice of the length assures that the transport along the edge state is ballistic [67] at the operating temperatures for our setup, typically of a few kelvin.

Conclusions. We investigated a phase-dependent nonlocal thermoelectricity in a topological Josephson junction coupled to a probe. We showed that an Andreev interferometric mechanism affects QPs and QHs differently resulting in a nonlocal thermoelectric response. We discussed the dependence of this mechanism over the junction length L and the coupling with the probe $|t|^2$. We estimated, with realistic parameters, a nonlocal Seebeck coefficient of a few μV/K at temperatures of a few kelvin. We underline that the provided estimations are quite conservative since the critical temperature T_C of the induced proximized gap is given by the critical temperature of the parent superconductors which is usually much higher, further increasing the nonlocal Seebeck coefficient which is proportional to the operating temperature. This thermoelectric effect is a consequence of the helical nature of the edge states [35] and can be used as evidence of the existence of these states in TI systems. Some of the experimental conditions for nonlocal Seebeck effect measurement are similar to the

proposed measurements of heat conductance in topological Josephson junctions [43,68], but here we discussed a mechanism which takes place in the absence of any magnetic field. The investigation of the nonlocal character in thermoelectrical coherent devices may open novel possibilities in thermal management and quantum sensing.

Acknowledgments. We acknowledge support from the CNR-CONICET cooperation program "Energy conversion in quantum nanoscale hybrid devices." We are sponsored by PIP-RD 20141216-4905 of CONICET, PICT-2017-2726 and PICT-2018-04536 from Argentina, as well as the Alexander von Humboldt Foundation, Germany and the ICTP-Trieste through a Simons associateship (L.A.). A.B. and F.T. acknowledge SNS-WIS joint laboratory QUANTRA. M.C. is supported by the Quant-Era project "Supertop." A.B. acknowledges the Royal Society through the International Exchanges between the UK and Italy (Grant No. IEC R2 192166).

[1] M. Partanen, K. Y. Tan, J. Govenius, R. E. Lake, M. K. Mäkelä, T. Tanttu, and M. Möttönen, Nat. Phys. **12**, 460 (2016) .
[2] A. Fornieri and F. Giazotto, Nat. Nanotechnol. **12**, 944 (2017).
[3] J. Senior, A. Gubaydullin, B. Karimi, J. Peltonen, J. Ankerhold, and J. Pekola, Commun. Phys. **3**, 40 (2020).
[4] N. R. Claughton and C. J. Lambert, Phys. Rev. B **53**, 6605 (1996).
[5] F. Mazza, S. Valentini, R. Bosisio, G. Benenti, V. Giovannetti, R. Fazio, and F. Taddei, Phys. Rev. B **91**, 245435 (2015).
[6] R. Sánchez, P. Burset, and A. L. Yeyati, Phys. Rev. B **98**, 241414(R) (2018).
[7] M. Kamp and B. Sothmann, Phys. Rev. B **99**, 045428 (2019).
[8] R. Hussein, M. Governale, S. Kohler, W. Belzig, F. Giazotto, and A. Braggio, Phys. Rev. B **99**, 075429 (2019).
[9] N. S. Kirsanov, Z. B. Tan, D. S. Golubev, P. J. Hakonen, and G. B. Lesovik, Phys. Rev. B **99**, 115127 (2019).
[10] S. S. Pershoguba and L. I. Glazman, Phys. Rev. B **99**, 134514 (2019).
[11] G. Marchegiani, A. Braggio, and F. Giazotto, Phys. Rev. Lett. **124**, 106801 (2020).
[12] F. Giazotto, P. Solinas, A. Braggio, and F. S. Bergeret, Phys. Rev. Appl. **4**, 044016 (2015).
[13] T. T. Heikkilä, R. Ojajärvi, I. J. Maasilta, E. Strambini, F. Giazotto, and F. S. Bergeret, Phys. Rev. Appl. **10**, 034053 (2018).
[14] C. Guarcello, A. Braggio, P. Solinas, G. P. Pepe, and F. Giazotto, Phys. Rev. Appl. **11**, 054074 (2019).
[15] G. Blasi, F. Taddei, V. Giovannetti, and A. Braggio, Phys. Rev. B **99**, 064514 (2019).
[16] F. Mazza, R. Bosisio, G. Benenti, V. Giovannetti, R. Fazio, and F. Taddei, New J. Phys. **16**, 085001 (2014).
[17] K. Yamamoto and N. Hatano, Phys. Rev. E **92**, 042165 (2015).
[18] F. Vischi, M. Carrega, P. Virtanen, E. Strambini, A. Braggio, and F. Giazotto, Sci. Rep. **9**, 3238 (2019).
[19] G. Marchegiani, A. Braggio, and F. Giazotto, Phys. Rev. B **101**, 214509 (2020).
[20] B. Scharf, A. Braggio, E. Strambini, F. Giazotto, and E. M. Hankiewicz, Commun. Phys. **3**, 198 (2020).
[21] P. Machon, M. Eschrig, and W. Belzig, Phys. Rev. Lett. **110**, 047002 (2013).
[22] A. Ozaeta, P. Virtanen, F. S. Bergeret, and T. T. Heikkila, Phys. Rev. Lett. **112**, 057001 (2014).
[23] S. Kolenda, C. Srgers, G. Fischer, and D. Beckmann, Phys. Rev. B **95**, 224505 (2017).
[24] D. S. Shapiro, D. E. Feldman, A. D. Mirlin, and A. Shnirman, Phys. Rev. B **95**, 195425 (2017).
[25] F. Keidel, S.-Y. Hwang, B. Trauzettel, B. Sothmann, and P. Burset, Phys. Rev. Res. **2**, 022019 (2020).
[26] D. Sanchez and R. Lopez, C. R. Phys. **17**, 1060 (2016).
[27] P. Virtanen and T. Heikkilä, J. Low Temp. Phys. **136**, 401 (2004).
[28] M. Titov, Phys. Rev. B **78**, 224521 (2008).
[29] Ph. Jacquod and R. S. Whitney, Europhys. Lett. **91**, 67009 (2010).
[30] M. S. Kalenkov, P. E. Dolgirev, and A. D. Zaikin, Phys. Rev. B **101**, 180505(R) (2020).
[31] J. Eom, C.-J. Chien, and V. Chandrasekhar, Phys. Rev. Lett. **81**, 437 (1998).
[32] Z. Jiang and V. Chandrasekhar, Phys. Rev. B **72**, 020502(R) (2005).
[33] A. Parsons, I. A. Sosnin, and V. T. Petrashov, Phys. Rev. B **67**, 140502(R) (2003).
[34] Z. B. Tan, A. Laitinen, N. S. Kirsanov, A. Galda, V. M. Vinokur, M. Haque, A. Savin, D. S. Golubev, G. B. Lesovik, and P. J. Hakonen, arXiv:2005.13286.
[35] G. Blasi, F. Taddei, L. Arrachea, M. Carrega, and A. Braggio, Phys. Rev. Lett. **124**, 227701 (2020).
[36] X.-L. Qi, and S.-C. Zhang, Rev. Mod. Phys. **83**, 1057 (2011).
[37] Y. Ando, J. Phys. Soc. Jpn. **82**, 102001 (2013).
[38] B. A. Bernevig, T. L. Hughes, and S.-C. Zhang, Science **314**, 1757 (2006).
[39] M. König, S. Wiedmann, C. Brüne, A. Roth, H. Buhmann, L. W. Molenkamp, X. L. Qi, and S.-C. Zhang, Science **318**, 766 (2007).
[40] F. Ronetti, M. Carrega, D. Ferraro, J. Rech, T. Jonckheere, T. Martin, and M. Sassetti, Phys. Rev. B **95**, 115412 (2017).
[41] L. Bours, B. Sothmann, M. Carrega, E. Strambini, E. M. Hankiewicz, and L. W. Molenkamp, F. Giazotto, Phys. Rev. Appl. **10**, 014027 (2018).
[42] G. Tkachov, P. Burset, B. Trauzettel, and E. M. Hankiewicz, Phys. Rev. B **92**, 045408 (2015).
[43] B. Sothmann and E. M. Hankiewicz, Phys. Rev. B **94**, 081407(R) (2016).
[44] S. Das and S. Rao, Phys. Rev. Lett. **106**, 236403 (2011).
[45] L. Liu, A. Richardella, I. Garate, Y. Zhu, N. Samarth, and C. T. Chen, Phys. Rev. B **91**, 235437 (2015).
[46] S. M. Hus, X. G. Zhang, G. D. Nguyen, W. Ko, A. P. Baddorf, Y. P. Chen, and A. P. Li, Phys. Rev. Lett. **119**, 137202 (2017).
[47] B. Voigtländer, V. Cherepanov, S. Korte, A. Leis, D. Cuma, S. Just, and F. Lüpke, Rev. Sci. Instrum. **89**, 101101 (2018).
[48] No voltage can be applied between the superconductors in order to avoid time-dependent dynamics (as a consequence of the Josephson relation).
[49] C. J. Lambert and R. Raimondi, J. Phys.: Condens. Matter **10**, 901 (1998).

[50] Ya. M. Blanter and M. Buttiker, Phys. Rep. **336**, 1 (2000).
[51] See Supplemental Material of Ref. [35] at http://link.aps.org/supplemental/10.1103/PhysRevLett.124.227701 for details of the calculations of the scattering coefficients.
[52] G. Benenti, G. Casati, K. Saito, and R. S. Whitney, Phys. Rep. **694**, 1 (2017).
[53] P. Roura-Bas, L. Arrachea, and E. Fradkin, Phys. Rev. B **98**, 195429 (2018).
[54] R. Sánchez, B. Sothmann, and A. N. Jordan, Phys. Rev. Lett. **114**, 146801 (2015).
[55] A. Mani and C. Benjamin, Phys. Rev. E **97**, 022114 (2018).
[56] The Onsager coefficients behave similarly to Figs. 3(a)–3(c) for any value of $|t|^2 \neq 0, 1$.
[57] P. Jacquod, R. S. Whitney, J. Meair, and M. Büttiker, Phys. Rev. B **86**, 155118 (2012).
[58] T. Engl, J. Kuipers, and K. Richter, Phys. Rev. B **83**, 205414 (2011).
[59] M. Tinkham, *Introduction to Superconductivity* (McGraw-Hill, New York, 1996).
[60] We took $\Delta(T) = \Delta_0 \tanh(1.74\sqrt{T_C/T - 1})$, an approximation good at 2% with respect to the self-consistent BCS result [7,59].
[61] A. Von Ettingshausen and W. Nernst, Ann. Phys. Chem. **265**, 343 (1886).
[62] K. Behnia and H. Aubin, Rep. Prog. Phys. **79**, 046502 (2016).
[63] Y. M. Zuev, W. Chang, and P. Kim, Phys. Rev. Lett. **102**, 096807 (2009).
[64] Z. Zhu, H. Yang, and B. Fauqué, Y. Kopelevich, and K. Behnia, Nat. Phys. **6**, 26 (2010).
[65] E. Bocquillon, R. S. Deacon, J. Wiedenmann, P. Leubner, T. M. Klapwijk, C. Brüne, K. Ishibashi, H. Buhmann, and L. W. Molenkamp, Nat. Nanotechnol. **12**, 137 (2017).
[66] S. Hart, H. Ren, T. Wagner, P. Leubner, M. Mühlbauer, C. Brüne, H. Buhmann, L. W. Molenkamp, and A. Yacoby, Nat. Phys. **10**, 638 (2014).
[67] S. Groenendijk, G. Dolcetto, and T. L. Schmidt, Phys. Rev. B **97**, 241406(R) (2018).
[68] B. Sothmann, F. Giazotto, and E. M. Hankiewicz, New J. Phys. **19**, 023056 (2017).